

Published in final edited form as:

Heart Rhythm. 2014 April ; 11(4): 697–706. doi:10.1016/j.hrthm.2013.12.032.

Hypokalemia Promotes Late Phase 3 Early Afterdepolarization and Recurrent Ventricular Fibrillation During Isoproterenol Infusion in Langendorff Perfused Rabbit Ventricles

Mitsunori Maruyama, MD, PhD, FHR^S*,†, Tomohiko Ai, MD, PhD*, Su-Kiat Chua, MD*, Hyung-Wook Park, MD, PhD*, Young-Soo Lee, MD, PhD*, Mark J. Shen, MD*, Po-Cheng Chang, MD*, Shien-Fong Lin, PhD*, and Peng-Sheng Chen, MD, FHR^S*

*Krannert Institute of Cardiology and the Division of Cardiology, Department of Medicine, Indiana University School of Medicine, Indianapolis, Indiana, USA

†Cardiovascular Center, Chiba-Hokusoh Hospital, Nippon Medical School, Chiba, Japan

Abstract

BACKGROUND—Hypokalemia and sympathetic activation are commonly associated with electrical storm (ES) in normal and diseased hearts. The mechanisms remain unclear.

OBJECTIVE—To test the hypothesis that late phase 3 early afterdepolarization (EAD) induced by I_{KATP} activation underlies the mechanisms of ES during isoproterenol infusion and hypokalemia.

METHODS—Intracellular calcium (Ca_i) and membrane voltage were optically mapped in 32 Langendorff-perfused normal rabbit hearts.

RESULTS—Repeated episodes of electrically-induced VF at baseline did not result in spontaneous VF (SVF). During isoproterenol infusion, SVF occurred in 1 of 15 hearts (7%) studied in normal extracellular potassium ($[K^+]_o$) (4.5 mmol/L), 3 of 8 hearts (38%) in 2.0 mmol/L $[K^+]_o$, 9 of 10 hearts (90%) in 1.5 mmol/L $[K^+]_o$, and 7 of 7 hearts (100%) in 1.0 mmol/L $[K^+]_o$ ($P < 0.001$). Optical mapping showed isoproterenol and hypokalemia enhanced Ca_i transient duration (Ca_iTD) and heterogeneously shortened action potential duration (APD) after defibrillation, leading to late phase 3 EAD and SVF. I_{KATP} blocker (glibenclamide, 5 μ mol/L) reversed the post-defibrillation APD shortening and suppressed recurrent SVF in all hearts studied despite no evidence of ischemia. Nifedipine reliably prevented recurrent VF when given before, but not after, the development of VF. I_{Kr} blocker (E-4031) and small conductance calcium activated potassium channel blocker (apamin) failed to prevent recurrent SVF.

© 2013 The Heart Rhythm Society. Published by Elsevier Inc. All rights reserved.

Address Reprint requests and correspondence: Dr. Peng-Sheng Chen, 1800 N. Capitol Ave, E475, Indianapolis, IN46202, Fax: 317-962-0588; Phone: 317-962-0145, chenpp@iupui.edu.

Publisher's Disclaimer: This is a PDF file of an unedited manuscript that has been accepted for publication. As a service to our customers we are providing this early version of the manuscript. The manuscript will undergo copyediting, typesetting, and review of the resulting proof before it is published in its final citable form. Please note that during the production process errors may be discovered which could affect the content, and all legal disclaimers that apply to the journal pertain.

Conflicts of interest: none

CONCLUSION—Beta-adrenergic stimulation and concomitant hypokalemia could cause non-ischemic activation of I_{KATP} , heterogeneous APD shortening and prolongation of Ca_T TD to provoke late phase 3 EAD, triggered activity and recurrent SVF. I_{KATP} inhibition may be useful in managing ES during resistant hypokalemia.

Keywords

ventricular fibrillation; electrical storm; hypokalemia; afterdepolarization; intracellular calcium; ATP-sensitive potassium channels

Introduction

Electrical storm (ES) describes a clinical condition characterized by multiple spontaneous ventricular fibrillation (SVF) episodes that necessitate repeated defibrillation. While ES usually occurs in patients with serious organic heart diseases, it is not rare in patients with structurally normal hearts and genetic arrhythmias such as Brugada and early repolarization syndromes. It is known that hypokalemia is a common trigger of ES.^{1, 2} Bansch et al³ reported that the recurrence risk of ES was highest in cardiomyopathic patients with hypokalemia and associated conditions such as diarrhea and vomiting. Hypokalemia is also associated with ES in structurally normal hearts and correction of hypokalemia can prevent the recurrent ventricular fibrillation (VF).^{4, 5} However, because rapid and safe correction of serum potassium is often difficult, additional drug therapy is often necessary to manage the ES. Sympathetic blockade, while not always effective, is commonly used in the management of ES.⁶ This clinical practice is consistent with the observation that sympathetic nerve activity is a direct and immediate trigger of ventricular tachycardia (VT) and ventricular fibrillation (VF).⁶ Hypokalemia alone does not enhance VF inducibility in normal dogs.⁷ However, sympathetic stimulation with isoproterenol and concomitant hypokalemia can induce VF in a rat model.⁸ Massive reactive sympathetic activation⁹ and the frequent use of epinephrine during fibrillation-defibrillation episodes¹⁰ may also induce hypokalemia in patients with ES, because beta adrenergic stimulation itself can elicit hypokalemia.¹¹ We have shown that heart failure in rabbits upregulate a small conductance calcium activated potassium current (I_{KAS}) and promote late phase 3 early afterdepolarization (EAD) leading to ES.^{12, 13} However, as far as we know, there are no animal models of ES in ventricles without chronic structural remodeling.

To test the importance of hypokalemia and sympathetic activation in the development of ES, we aim to develop a model of ES in normal rabbit ventricles in the presence of hypokalemia during isoproterenol infusion. This animal model is then used to test the hypothesis that late phase 3 EAD is important in the recurrence of SVF after defibrillation, similar to that occurs after electrical shocks in normal canine atria.¹⁴ We then tested a third hypothesis that glibenclamide, an I_{KATP} blocker, is effective in preventing ES in this model.

Methods

The details of experimental methods and protocol are available at Online Data Supplement. The isolated rabbit hearts (n=32) were perfused to maintain a perfusion pressure above 70

mmHg throughout the study. Intracellular calcium (Ca_i) and membrane voltage (V_m) were simultaneously mapped using optical mapping techniques as described previously.¹²

VF was electrically-induced and allowed to persist for 3 min under maintained coronary perfusion, followed by defibrillation. The set of 3-min VF and 1-min observational period was repeated up to 5 times unless SVF occurred. VF induction and defibrillation were repeated in control and during isoproterenol infusion (0.3 $\mu\text{mol/L}$) to determine the role of beta-adrenergic stimulation in the action potential duration (APD) shortening after VF episodes ($n=5$). Thereafter, we tested various levels of $[K^+]_o$ (4.5, 2.0, 1.5, and 1.0 mmol/L) during beta-adrenergic stimulation ($n=17$). In an additional 10 hearts, pharmacological interventions were applied to identify the mechanism of the post-defibrillation APD shortening during beta-adrenergic stimulation at the normal $[K^+]_o$ level. APD was measured at 50% (APD₅₀) and 80% (APD₈₀) repolarization. Continuous variables were expressed as mean \pm SEM. $P < 0.05$ was considered statistically significant.

Results

A Model of ES in Normal Ventricles

We successfully developed a model of ES in these normal ventricles. We defined ES as multiple (3) consecutive episodes of SVF recurrences after initial successful defibrillation. In control, no SVF was observed with 5 attempts of the induced VF-defibrillation episodes. During isoproterenol infusion, SVF occurred in 1 of 15 hearts (7%) studied in normal $[K^+]_o$ (4.5 mmol/L), 3 of 8 hearts (38%) in 2.0 mmol/L $[K^+]_o$, 9 of 10 hearts (90%) in 1.5 mmol/L $[K^+]_o$, and 7 of 7 hearts (100%) in 1.0 mmol/L $[K^+]_o$ ($P < 0.001$). The SVF episodes evolved into ES in 0 of 15 hearts (0%), 1 of 8 hearts (13%), 8 of 10 hearts (80%), and 6 of 7 hearts (86%) studied in the $[K^+]_o$ of 4.5 mmol/L, 2.0 mmol/L, 1.5 mmol/L, and 1.0 mmol/L, respectively ($P < 0.001$). The ES developed after the $2.7 \pm 1.1^{\text{th}}$ episodes of electrically-induced VF. In the majority of ES (13/15 hearts, 87%), VTs (cycle length: 345 ± 10 ms) were observed between the SVF episodes. Figure 1A shows a typical example of ES observed under isoproterenol infusion in 1.0 mmol/L $[K^+]_o$. First, a pacing-induced VF was successfully defibrillated. VT followed the successful defibrillation, and then SVF occurred. Despite multiple attempts of defibrillation, all subsequent shocks seemed to fail to defibrillate the SVF on pseudo-ECG. However, optical recordings revealed that each shock actually terminated the SVF successfully, followed by immediate recurrences of SVF. A large difference between APD and Ca_i transient duration (Ca_i TD) was noted during the ES. The initiation of the SVF was associated with a short-coupled ventricular ectopy (Figure 1B). The coupling interval of the ectopic beat that initiated SVF was significantly shorter than that of the ectopic beat not initiating SVF (150 ± 5 ms versus 239 ± 6 ms, $P < 0.001$). There was no apparent QRS or T wave alternans during VT before transition to SVF. Repeated defibrillation (5 ± 2 successful defibrillation, shock intensity: 177 ± 6 V) alone terminated ES in only 2 hearts (14%).

Post-defibrillation VT (Online Figure I) was observed only during isoproterenol infusion and more frequently with a lower $[K^+]_o$ (VT incidence: 17%, 33%, 60%, and 71% at $[K^+]_o$ of 4.5, 2.0, 1.5, and 1.0 mmol/L, respectively). Spontaneous Ca_i elevations preceded the VT

beats, and the VT was effectively suppressed by 10 $\mu\text{mol/L}$ nifedipine but not by ventricular overdrive pacing.

Post-Defibrillation Action Potential Triangulation during Beta-Adrenergic Stimulation

In control, APD was modestly shortened after defibrillation of 3-min electrically-induced VF, which is likely due to dependence of APD on the entire activation history (i.e. short-term memory effect). However, iteration of VF episodes did not further shorten the post-defibrillation APD, probably because the memory of the APD reached a steady state. This is consistent with our previous results which showed that no marked APD shortening occurred after defibrillation in non-failing hearts.^{12, 13} In contrast, the post-defibrillation APD was progressively shortened as VF episodes were repeated during isoproterenol infusion (0.3 $\mu\text{mol/L}$) even using normal hearts (Figure 2A). The magnitude of the post-defibrillation APD shortening at 50% and 80% repolarization were similar in control, while repeated VF episodes during isoproterenol infusion accelerated early repolarization of the post-defibrillation beats, resulting in more shortening of APD_{50} than APD_{80} and triangulation of the action potential (AP) in some epicardial sites (Figure 2B and 2C).

Non-Ischemic Activation of ATP-Sensitive Potassium Current

Since the AP triangulation is often observed in an ischemic condition which causes I_{KATP} activation, we tested the effect of an I_{KATP} blocker, glibenclamide (5 $\mu\text{mol/L}$, $n=6$). The dominant frequency of pseudo-ECG during VF decreased after administration of glibenclamide (13.7 ± 2.1 Hz to 8.3 ± 0.9 Hz, $P<0.005$). After defibrillation, glibenclamide prolonged the APD and abolished the post-defibrillation AP triangulation (Figure 3A), suggesting activation of I_{KATP} as the mechanism of the APD shortening. However, under maintained coronary perfusion, a significant myocardial ischemia could not be detected after multiple VF episodes by measuring lactate concentrations in coronary sinus effluent (pre-VF: 0.36 ± 0.16 mmol/L versus post-VF: 0.36 ± 0.15 mmol/L, $P=0.947$). The reversal of the post-defibrillation APD shortening was unlikely to result from a non-specific effect of glibenclamide on other ionic currents such as cystic fibrosis transmembrane regulator chloride current (I_{CFTR}) which is known to be activated by isoproterenol and blocked by a higher dose of glibenclamide, since a potent inhibitor of I_{CFTR} , $\text{CFTR}_{\text{inh-172}}$ (10 $\mu\text{mol/L}$, $n=5$)¹⁵ did not affect the post-defibrillation APD (Figure 3B). Also, I_{KAS} blocker, apamin (100 nmol/L, $n=5$) did not prolong the post-defibrillation APD. Thus I_{KAS} plays a role only in failing hearts,¹² but not in the post-defibrillation APD shortening during beta-adrenergic stimulation.

Mechanisms of ES Induced by Hypokalemia and Isoproterenol Infusion

We analyzed simultaneous V_m and Ca_i optical recordings to identify how hypokalemia promoted the occurrences of SVF and ES. Figure 4 shows the effects of repeated episodes of induced-VF on post-defibrillation APD and Ca_iTD . In control (normal $[\text{K}^+]_o$, no isoproterenol), multiple VF episodes homogeneously shortened APDs of post-defibrillation beats. Ca_iTD was shortened by 10 to 20% corresponding to the APD shortening. As stated above, APD_{50} was progressively shortened during isoproterenol infusion with the AP shape being triangulated. In contrast, $\text{Ca}_i\text{TD}_{50}$ was not altered, and the difference between

Ca_iTD_{50} and APD_{50} ($Ca_iTD_{50}-APD_{50}$) was increased in the area with the AP triangulation. When $[K^+]_o$ was reduced, pre-VF APD was prolonged. However, the APD was shortened again after VF episodes in some sites, thereby enhancing the APD dispersion. In addition, Ca_iTD was progressively prolonged after induced-VF episodes by reduced $[K^+]_o$ and isoproterenol, leading to a larger $Ca_iTD_{50}-APD_{50}$. Of initial 5 hearts, SVF occurred during isoproterenol infusion at a low $[K^+]_o$ after the 2nd induced-VF in one heart, and after the 5th induced-VF in 4 hearts. The increased $Ca_iTD_{50}-APD_{50}$ and APD dispersion were associated with the recurrent SVF.

Figure 5A shows an example of SVF after defibrillation. SVF occurred with a short-coupled ventricular ectopy (filled circle) similar to that seen in ES of human patients.¹⁶ A focal activation arising from the anterior surface of the left ventricle (site (a)) preceded the QRS onset of the first SVF beat by 34 ms, indicating that the SVF originated from this site. The AP triangulation was seen only around the site of origin with increased APD dispersion. Notably, a high V_m gradient area secondary to the heterogeneous APD coincided with a functional block line for the initial SVF beat, but not with the site of origin where

$Ca_iTD_{50}-APD_{50}$ was increased. These findings suggest that Ca_i -dependent phase 3 EADs may underlie the mechanism of the first SVF beat, but the increased APD heterogeneity and conduction block facilitated the development of reentry and wavebreak that promoted the development of SVF. In spite of a large V_m gradient, there was no evidence of phase 2 reentry. Furthermore, a spatial distribution of dominant frequency during this SVF episode displayed a focal source pattern with the highest dominant frequency site near the site where SVF started, indicating that repetitive focal activations as well as reentry both contributed to the maintenance of the SVF in this case.

We acquired optical data during 59 episodes of SVF. Sixteen episodes of the SVF were initiated by a focal activity arising from the mapped field. In 11 of 16 (69%) episodes, the earliest site for the focal activation had the maximal or submaximal value of $Ca_iTD_{50}-APD_{50}$ (Figure 5B).

Pharmacological Interventions on ES

We sought a novel therapeutic target for controlling ES by testing the effect of pharmacological interventions. Since I_{KATP} activation is responsible for post-defibrillation APD shortening during sympathetic stimulation, we examined the effect of 5 $\mu\text{mol/L}$ glibenclamide on ES ($n=4$). Of note, glibenclamide diminished $Ca_iTD_{50}-APD_{50}$ (128 ± 15 ms to 53 ± 12 ms, $P<0.05$) and terminated all the ES episodes (Figure 6). In 7 hearts, we transiently increased the coronary perfusion pressure to determine if a relative ischemia that could not be detected by the lactate assay contributed to the ES. The increase in the perfusion pressure by 59 ± 5 mmHg did not change the APD_{50} and never terminated the ES, confirming that I_{KATP} activation cannot be attributed to ischemia in this model. Glibenclamide did not terminate VT except in one heart where VT stopped spontaneously 42 sec after termination of ES with glibenclamide (Figure 6). The remaining VT was suppressed with a selective L-type Ca^{2+} channel blocker, nifedipine (10 $\mu\text{mol/L}$, Online Figure I).

Because Ca_i overload seems essential for the development of SVF, we also tested the effect of nifedipine (10 $\mu\text{mol/L}$, $n=8$) on ES. When nifedipine was given before VF induction (pre-treatment group, $n=3$), VT and SVF were prevented even under isoproterenol infusion at 1.0 mmol/L $[K^+]_o$. When pre-treated with nifedipine, APD_{50} was still shortened in some sites after VF episodes ($-57 \pm 9\%$ of the pre-VF values after 5th VF episode), but concomitant shortening of Ca_i TD kept Ca_i TD₅₀- APD_{50} small (11 ± 4 ms, Figure 7A). In contrast, responses to nifedipine varied when nifedipine was administered after ES developed (post-treatment group, $n=5$). Nifedipine suppressed VT/SVF in one heart that had a long period of VT prior to SVF recurrence (Figure 7B). The maximal Ca_i TD₅₀- APD_{50} was reduced as a result of shortened Ca_i TD by nifedipine (124 ms to 32 ms). The other 4 hearts showed immediate recurrences of SVF before nifedipine treatment (upper panel in Figure 7C). Nifedipine was not effective in 2 of 4 hearts (Ca_i TD₅₀- APD_{50} : 101 ± 5 ms to 95 ± 11 ms, $P=0.50$). In the remaining 2 hearts, nifedipine inhibited post-defibrillation VT, which prolonged the interval from defibrillation to SVF recurrence. In this case, repeated defibrillation finally terminated the ES (lower panel in Figure 7C). The suppression of post-defibrillation VT allowed Ca_i overload to be more alleviated during the slower escape rhythm, which is the likely mechanism underlying termination of ES. Remarkably, glibenclamide terminated the ES resistant to nifedipine treatment ($n=2$, Online Figure II).

APD shortening was a critical component for ES. Therefore, we tested the effect of I_{Kr} blockade with E-4031 (1 $\mu\text{mol/L}$, $n=4$), because most of class I and III antiarrhythmic drugs used in the clinical practice prolong APD mainly by blocking I_{Kr} . Contrary to our expectation, E-4031 failed to prolong APD_{50} and to terminate the ES (Figure 8). E-4031 did not change the maximal Ca_i TD₅₀- APD_{50} . E-4031 also failed to suppress VT between SVF episodes. However, rescue dosage of glibenclamide (5 $\mu\text{mol/L}$) abolished the SVF in all hearts refractory to I_{Kr} blockade.

Discussion

Mechanisms of SVF in Normal Hearts with Hypokalemia and Beta-Adrenergic Stimulation

Because beta-adrenergic stimulation can by itself induce hypokalemia,^{11, 17} it is difficult to test the influence of *hypokalemia* on isoproterenol proarrhythmia in vivo. Langendorff perfusion allowed us to control the potassium levels in the perfusate. With this method, we showed that isoproterenol infusion and concomitant hypokalemia could cause ES in normal rabbit ventricles. During beta-adrenergic stimulation, prolonged VF episodes increased APD dispersion after defibrillation and elicited short-coupled ectopic beats, both of which contributed to SVF. Although the SVF arose from the site where APD was shortened, the APD shortening alone did not cause the SVF. Hypokalemia enhances calcium entry into cardiomyocytes during VF by suppressing sodium-potassium ATPase activity and consequent reverse mode of sodium-calcium exchanger.¹⁸ The Ca_i overload resulted in prolongation of Ca_i TD, which was necessary for the development of SVF. One may assume that heterogeneous APD shortening cause phase 2 reentry,¹⁹ but there was no evidence of phase 2 reentry in our model. Rather, APD dispersion was related to the formation of unidirectional conduction block (Figure 5). Although a positive V_m slope representing the late phase 3 EAD did not always precede the upstroke of triggered activities, the maximal

Ca_iTD_{50} -APD₅₀ predicted the origin for the first SVF beat better than the minimal APD₅₀ (Figure 5B). This strongly supports late phase 3 EAD as the underlying mechanism in which persistence of elevated Ca_i with accelerated repolarization promotes inward sodium-calcium exchanger currents. In our experimental setting, optical signal from one pixel reflects activities of hundreds of cardiomyocytes, which may obscure the deflection of late phase 3 EAD in some cases by an averaging effect.

Role of Beta-Adrenergic Stimulation in I_{KATP} Activation

With beta-adrenergic stimulation, APD₅₀ was more shortened than APD₈₀ after VF episodes, resulting in AP triangulation. The AP triangulation disappeared with 5 μ mol/L glibenclamide, which mainly blocks I_{KATP} at this concentration. Glibenclamide also blocks I_{CFTR} and I_{Kr} at higher concentrations.²⁰ Because we observed no effects of I_{CFTR} or I_{Kr} blockade on the shortened APD, we excluded major contribution of these ionic currents to the effects of glibenclamide. Therefore, we conclude that I_{KATP} activation is responsible for the AP triangulation. A high metabolic demand with rapid activation during VF under beta-adrenergic stimulation might reduce intracellular ATP and activate the I_{KATP} in spite of a negligible lactate production. K_{ATP} channel was thought to open only when exposed to severe metabolic stress such as ischemia, since a relatively low level of intracellular ATP can inhibit the activation of I_{KATP} in cell-free, inside-out patch-clamp studies.²¹ However, ATP sensitivity of K_{ATP} channel is lower in intact cells than that of excised inside-out patches because of the presence of intracellular cofactors including ADP, G-protein, H^+ , extracellular adenosine,²² and membrane phospholipid.²³ Also, beta-adrenergic-induced cAMP-dependent phosphorylation of channel proteins activates K_{ATP} channel.²⁴ Recent evidence from mice lacking Kir6.2 that encodes pore-forming subunit of cardiac K_{ATP} channel demonstrated that isoproterenol-induced APD shortening observed in wild-type mice was absent in Kir6.2-knockout mice, indicating that stress by beta-adrenergic stimulation alone can activate I_{KATP} .²⁵ Furthermore, prolonged rapid ventricular pacing (30 min) was reported to induce non-ischemic activation of I_{KATP} .²⁶ Taken together, rapid activations during VF under beta-adrenergic stimulation would activate I_{KATP} even in the absence of ischemia. Although VF in *in-vivo* hearts is inevitably followed by myocardial ischemia that activates I_{KATP} , our results uncovered physiological impacts of sympathetic activation during prolonged VF per se. Insufficient coronary perfusion during cardiopulmonary resuscitation would further promote I_{KATP} activation and Ca_i overload, which might shorten the VF duration necessary for the development of recurrent VF. It is true that APD shortening by I_{KATP} activation protects cardiomyocytes by limiting calcium entry, especially during severe metabolic stress.²⁵ However, our results indicate that excessive APD shortening due to I_{KATP} activation can be critically arrhythmogenic and exacerbates Ca_i overload by facilitating VF sustenance. A recent experimental study using cardiomyopathic human hearts also has shown that I_{KATP} blockade has an antiarrhythmic effect on VF even in the presence of myocardial ischemia.²⁷

Intervening VTs in ES

Although SVF recurred during post-defibrillation VT in a majority of ES episodes, SVF also occurred in the absence of VT (i.e. during escape rhythm), indicating that VT is not prerequisite for SVF recurrence. It follows that degeneration of VT into VF²⁸ is an unlikely

mechanism of SVF in this model. We found that a late phase 3 EAD is responsible for SVF, while a delayed afterdepolarization was a likely mechanism of the post-defibrillation VT since spontaneous Ca_i elevations occurred before the VT beats (Online Figure 1). Ca_i overload is essential for both SVF and post-defibrillation VT; however, APD shortening with I_{KATP} activation is also required for the development of SVF. Recovery from the APD shortening is time-dependent and influenced by the activation cycle length during the post-defibrillation period (Online Figure III). A higher heart rate during VT seems to promote SVF occurrence by preventing sufficient recovery of APD shortening and Ca_i overload. Suppression of VT with nifedipine both reduced the heart rate and reduced Ca^{2+} entry into the cells, allowing the heart to better recover from Ca_i overload and the APD shortening during the post-defibrillation periods, and terminated ES as long as Ca_iTD_{50} -APD₅₀ sufficiently decreased.

Clinical Implications

Even if patients have normokalemia at baseline, a high sympathetic tone during ES may cause hypokalemia through beta 2 adrenoceptor stimulation.¹¹ It is imperative to maintain a high serum potassium level to prevent ES especially when catecholamine is administered. If a quick restoration of serum potassium level is difficult, I_{KATP} inhibition may be useful in managing this life-threatening condition. Amiodarone, the first-line therapy for ES₁ and shock-resistant VF²⁹ may in part achieve its antiarrhythmic effects by inhibiting sarcolemmal I_{KATP} ³⁰ in addition to its beta-blocking effect.

Conclusion

Despite maintained tissue perfusion, prolonged episodes of VF under beta-adrenergic activation and hypokalemia could cause heterogeneous APD abbreviation due to non-ischemic I_{KATP} activation and Ca_iTD prolongation, leading to late phase 3 EAD, triggered activity and SVF. Importantly, once the heart develops recurrent VF, DC shocks alone may not be sufficient to restore normal rhythm. Rapid correction of hypokalemia and I_{KATP} inhibition would be useful in controlling ES.

Supplementary Material

Refer to Web version on PubMed Central for supplementary material.

Acknowledgments

Sources of Funding

This study was supported in part by National Institutes of Health grants P01 HL78931, R01 71140 and R21HL106554; Grant-in-Aid for Scientific Research 24591076 from the Ministry of Education, Culture, Sports, Science and Technology of Japan (to Dr. Maruyama), a Heart Rhythm Society Fellowship in Cardiac Pacing and Electrophysiology (to Dr. Shen), a Medtronic- Zipes endowment (to Dr. Chen) and the Indiana University Health - Indiana University School of Medicine Strategic Research Initiative. The content is solely the responsibility of the authors and does not necessarily represent the official views of the National Institutes of Health.

We thank Jian Tan for his technical assistance for lactate measurement.

ABBREVIATIONS

AP	action potential
APD	action potential duration
Ca_i	intracellular calcium
Ca_iTD	duration of Ca _i transient
EAD	early afterdepolarization
ES	electrical storm
I_{CFTR}	cystic fibrosis transmembrane regulator chloride current
I_{KAS}	small conductance calcium activated potassium current
I_{KATP}	ATP-sensitive potassium current
I_{Kr}	rapid component of delayed rectifier potassium current
[K⁺]_o	extracellular potassium concentration
SVF	spontaneous ventricular fibrillation
VF	ventricular fibrillation
V_m	membrane voltage
VT	ventricular tachycardia

References

1. Credner SC, Klingenheben T, Mauss O, Sticherling C, Hohnloser SH. Electrical storm in patients with transvenous implantable cardioverter-defibrillators: Incidence, management and prognostic implications. *J Am Coll Cardiol.* 1998; 32:1909–1915. [PubMed: 9857871]
2. Israel CW, Barold SS. Electrical storm in patients with an implanted defibrillator: A matter of definition. *Ann.Noninvasive.Electrocardiol.* 2007; 12:375–382. [PubMed: 17970963]
3. Bansch D, Bocker D, Brunn J, Weber M, Breithardt G, Block M. Clusters of ventricular tachycardias signify impaired survival in patients with idiopathic dilated cardiomyopathy and implantable cardioverter defibrillators. *J Am Coll Cardiol.* 2000; 36:566–573. [PubMed: 10933373]
4. Araki T, Konno T, Itoh H, Ino H, Shimizu M. Brugada syndrome with ventricular tachycardia and fibrillation related to hypokalemia. *Circ J.* 2003; 67:93–95. [PubMed: 12520160]
5. Myojo T, Sato N, Nimura A, et al. Recurrent ventricular fibrillation related to hypokalemia in early repolarization syndrome. *Pacing Clin Electrophysiol.* 2012; 35:e234–e238. [PubMed: 22734973]
6. Nademanee K, Taylor R, Bailey WE, Rieders DE, Kosar EM. Treating electrical storm: Sympathetic blockade versus advanced cardiac life support-guided therapy. *Circulation.* 2000; 102:742–747. [PubMed: 10942741]
7. Vera Z, Janzen D, Desai J. Acute hypokalemia and inducibility of ventricular tachyarrhythmia in a nonischemic canine model. *Chest.* 1991; 100:1414–1420. [PubMed: 1935303]
8. Guideri G. Death in ventricular fibrillation induced by isoproterenol in DOCA-salt pretreated rats preceded by changes in myocardial electrolytes. *Life Sci.* 1983; 33:1353–1362. [PubMed: 6621246]
9. Zhou S, Jung BC, Tan AY, et al. Spontaneous stellate ganglion nerve activity and ventricular arrhythmia in a canine model of sudden death. *Heart Rhythm.* 2008; 5:131–139. [PubMed: 18055272]

10. Korte T, Jung W, Ostermann G, et al. Hospital readmission after transvenous cardioverter/defibrillator implantation; a single centre study. *Eur Heart J.* 2000; 21:1186–1191. [PubMed: 10924302]
11. Prystowsky EN, Browne KF, Zipes DP. Intracardiac recording by catheter electrode of accessory pathway depolarization. *J.Am.Coll.Cardiol.* 1983; 1:468–470. [PubMed: 6826957]
12. Chua S-K, Chang P-C, Maruyama M, et al. Small-conductance calcium-activated potassium channel and recurrent ventricular fibrillation in failing rabbit ventricles. *Circ Res.* 2011
13. Ogawa M, Morita N, Tang L, et al. Mechanisms of recurrent ventricular fibrillation in a rabbit model of pacing-induced heart failure. *Heart Rhythm.* 2009; 6:784–792. [PubMed: 19467505]
14. Burashnikov A, Antzelevitch C. Reinduction of atrial fibrillation immediately after termination of the arrhythmia is mediated by late phase 3 early afterdepolarization-induced triggered activity. *Circulation.* 2003; 107:2355–2360. [PubMed: 12695296]
15. Mochizuki M, Yano M, Oda T, et al. Scavenging free radicals by low-dose carvedilol prevents redox-dependent Ca^{2+} leak via stabilization of ryanodine receptor in heart failure. *J.Am.Coll.Cardiol.* 2007; 49:1722–1732. [PubMed: 17448375]
16. Chinushi M, Iijima K, Sato A, Furushima H. Short-coupling premature ventricular complexes from the left ventricle triggered isoproterenol-resistant electrical storm in a patient with Brugada syndrome. *Heart Rhythm.* 2013; 10:916–920. [PubMed: 23333720]
17. Vaughan WEM. Delayed ventricular repolarization as an anti-arrhythmic principle. *Eur Heart J.* 1985; 6(Suppl D):145–149. [PubMed: 2417849]
18. Tribulova N, Manoach M, Varon D, Okruhlicova L, Zinman T, Shainberg A. Dispersion of cell-to-cell uncoupling precedes low K^{+} -induced ventricular fibrillation. *Physiol Res.* 2001; 50:247–259. [PubMed: 11521735]
19. Cha YM, Birgersdotter-Green U, Wolf PL, Peters BB, Chen PS. The mechanism of termination of reentrant activity in ventricular fibrillation. *Circ Res.* 1994; 74:495–506. [PubMed: 8118958]
20. Rosati B, Rocchetti M, Zaza A, Wanke E. Sulfonylureas blockade of neural and cardiac HERG channels. *FEBS Lett.* 1998; 440:125–130. [PubMed: 9862440]
21. Billman GE. The cardiac sarcolemmal ATP-sensitive potassium channel as a novel target for anti-arrhythmic therapy. *Pharmacol Ther.* 2008; 120:54–70. [PubMed: 18708091]
22. Hiraoka M. Pathophysiological functions of ATP-sensitive K^{+} channels in myocardial ischemia. *Jpn Heart J.* 1997; 38:297–315. [PubMed: 9290566]
23. Baukrowitz T, Schulte U, Oliver D, et al. PIP2 and PP as determinants for ATP inhibition of K_{ATP} channels. *Science.* 1998; 282:1141–1144. [PubMed: 9804555]
24. Achleitner U, Wenzel V, Strohmenger HU, et al. The effects of repeated doses of vasopressin or epinephrine on ventricular fibrillation in a porcine model of prolonged cardiopulmonary resuscitation. *Anesth Analg.* 2000; 90:1067–1075. [PubMed: 10781454]
25. Zingman LV, Hodgson DM, Bast PH, et al. Kir6.2 is required for adaptation to stress. *Proc Natl Acad Sci USA.* 2002; 99:13278–13283. [PubMed: 12271142]
26. Koning MM, Gho BC, van KE, Opstal RL, Duncker DJ, Verdouw PD. Rapid ventricular pacing produces myocardial protection by nonischemic activation of $\text{K}_{\text{ATP}}^{+}$ channels. *Circulation.* 1996; 93:178–186. [PubMed: 8616925]
27. Farid TA, Nair K, Masse S, et al. Role of K_{ATP} channels in the maintenance of ventricular fibrillation in cardiomyopathic human hearts. *Circ Res.* 2011; 109:1309–1318. [PubMed: 21980123]
28. Weiss JN, Garfinkel A, Karagueuzian HS, Qu Z, Chen PS. Chaos and the transition to ventricular fibrillation: A new approach to antiarrhythmic drug evaluation. *Circulation.* 1999; 99:2819–2826. [PubMed: 10351978]
29. Dorian P, Cass D, Schwartz B, Cooper R, Gelaznikas R, Barr A. Amiodarone as compared with lidocaine for shock-resistant ventricular fibrillation. *N Engl J Med.* 2002; 346:884–890. [PubMed: 11907287]
30. Sato T, Takizawa T, Saito T, Kobayashi S, Hara Y, Nakaya H. Amiodarone inhibits sarcolemmal but not mitochondrial K_{ATP} channels in guinea pig ventricular cells. *J Pharmacol Exp Ther.* 2003; 307:955–960. [PubMed: 14534361]

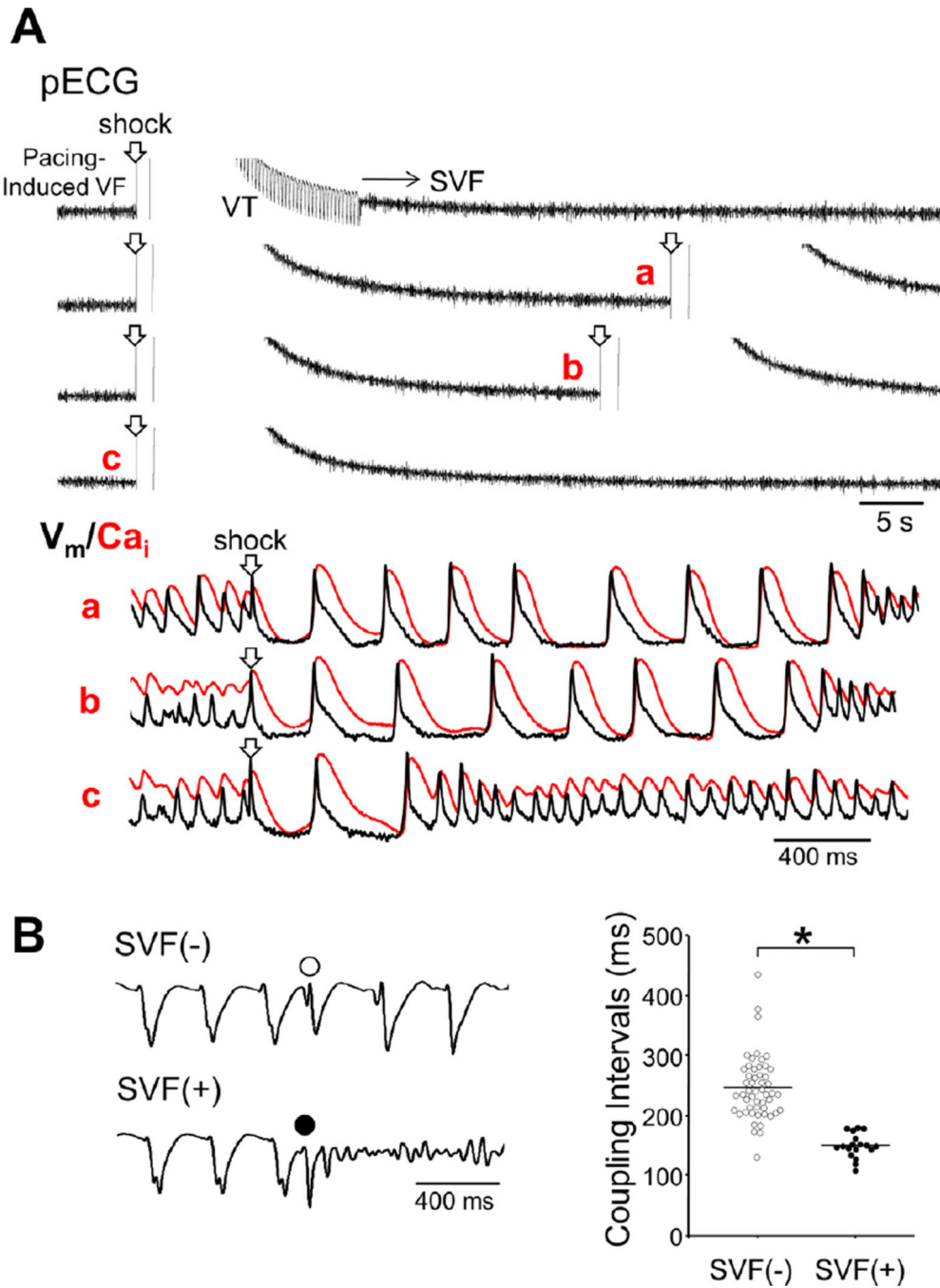


Figure 1.

SVF and ES. **(A)** (upper panels) Pseudo-ECG (pECG) during a typical example of ES. SVF followed post-defibrillation VT. All subsequent shocks seem to fail on the ECG, which is compatible with shock-resistant VF. Simultaneous recordings of V_m and Ca_i obtained at time points indicated in alphabets on ECG revealed that all the shocks successfully defibrillated, but SVF emerged immediately. **(B)** Left panel shows pECGs for ventricular ectopy with (filled circle) and without (unfilled circle) a transition to VF. Right panel shows scatterplot for the coupling interval of ventricular ectopy with and without VF induction. * $P < 0.001$.

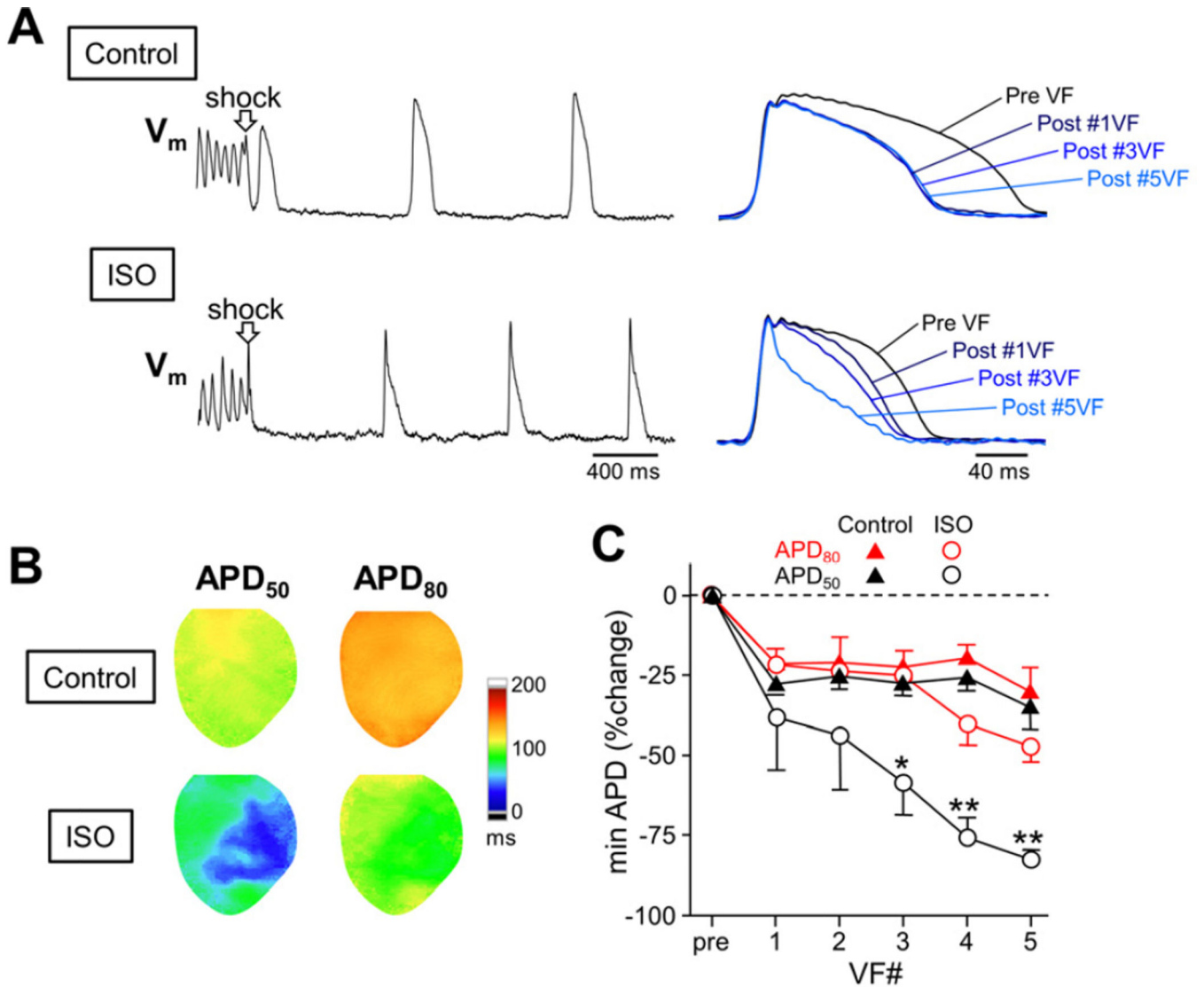


Figure 2.

Post-defibrillation APD shortening during sympathetic stimulation. **(A)** Optical V_m signals during successful defibrillation in control (upper panel) and during isoproterenol infusion (ISO, lower panel). Right panels show superimposed optical APs for the beat before VF and immediately after defibrillation of first, third and fifth 3-min VFs. **(B)** APD₅₀ and APD₈₀ maps for the post-VF beat in control and during ISO. Optical V_m tracings in panel (A) were taken at the minimal APD₅₀ site. **(C)** Alteration in mean \pm SEM values of APD₅₀ (black) and APD₈₀ (red) for the post-VF beat as VF induction-defibrillation sequences were repeated in control (triangles) and during ISO (circles) (n=5). * P <0.05; ** P <0.01 versus APD₈₀ of the counterpart during ISO.

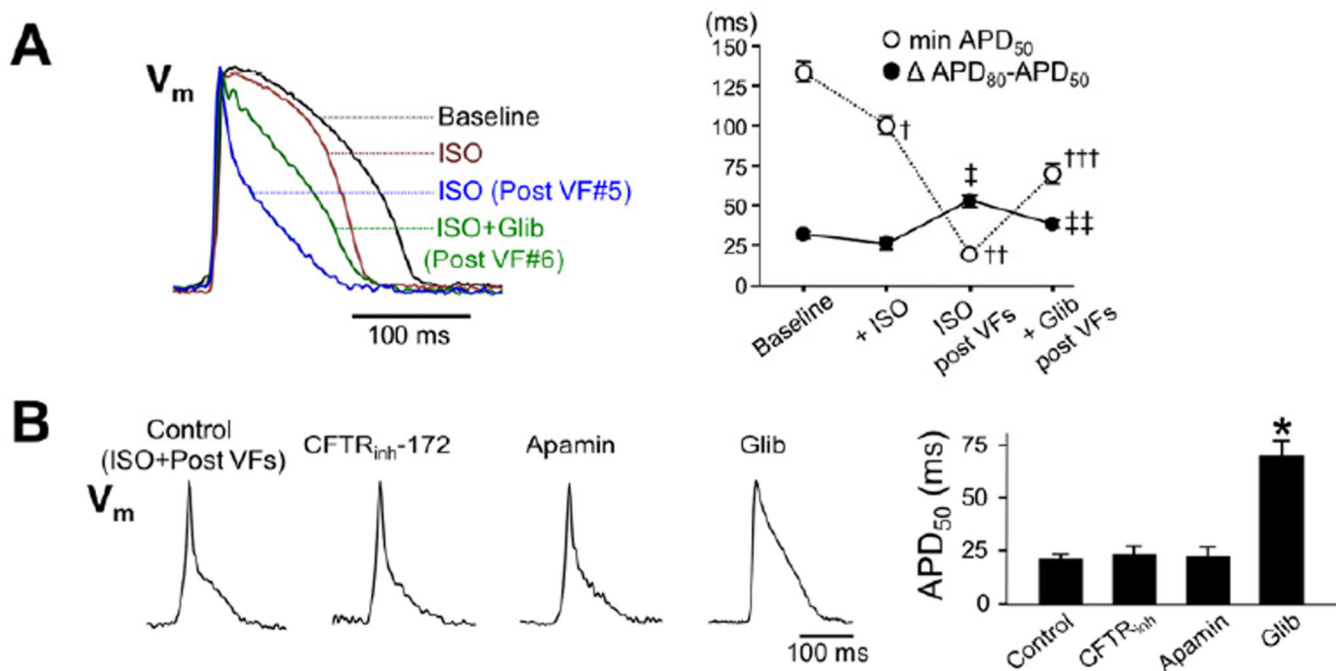


Figure 3.

I_{KATP} activation with VF and sympathetic stimulation. **(A)** (Left panel) Shown are superimposed optical APs at baseline, during isoproterenol (ISO), for the 1st beat after defibrillation of 5th induced-VF during ISO (ISO post-VFs), and for the 1st beat after defibrillation of 6th induced-VF during ISO plus glibenclamide (Glib). (Right panel) Changes in mean \pm SEM values of the minimal APD_{50} and the maximal $Ca_iTD_{50}-APD_{50}$ ($n=6$). $\ddagger P < 0.001$ versus ISO; $\ddagger\ddagger P < 0.005$ versus ISO post-VFs; $\dagger P < 0.005$ versus baseline; $\dagger\dagger P < 0.001$ versus ISO; $\dagger\dagger\dagger P < 0.001$ versus ISO post-VFs. **(B)** Effects of $CFTR_{inh-172}$ ($n=5$), apamin ($n=5$), and Glib ($n=6$) on AP shape and APD_{50} . $*P < 0.001$ versus control.

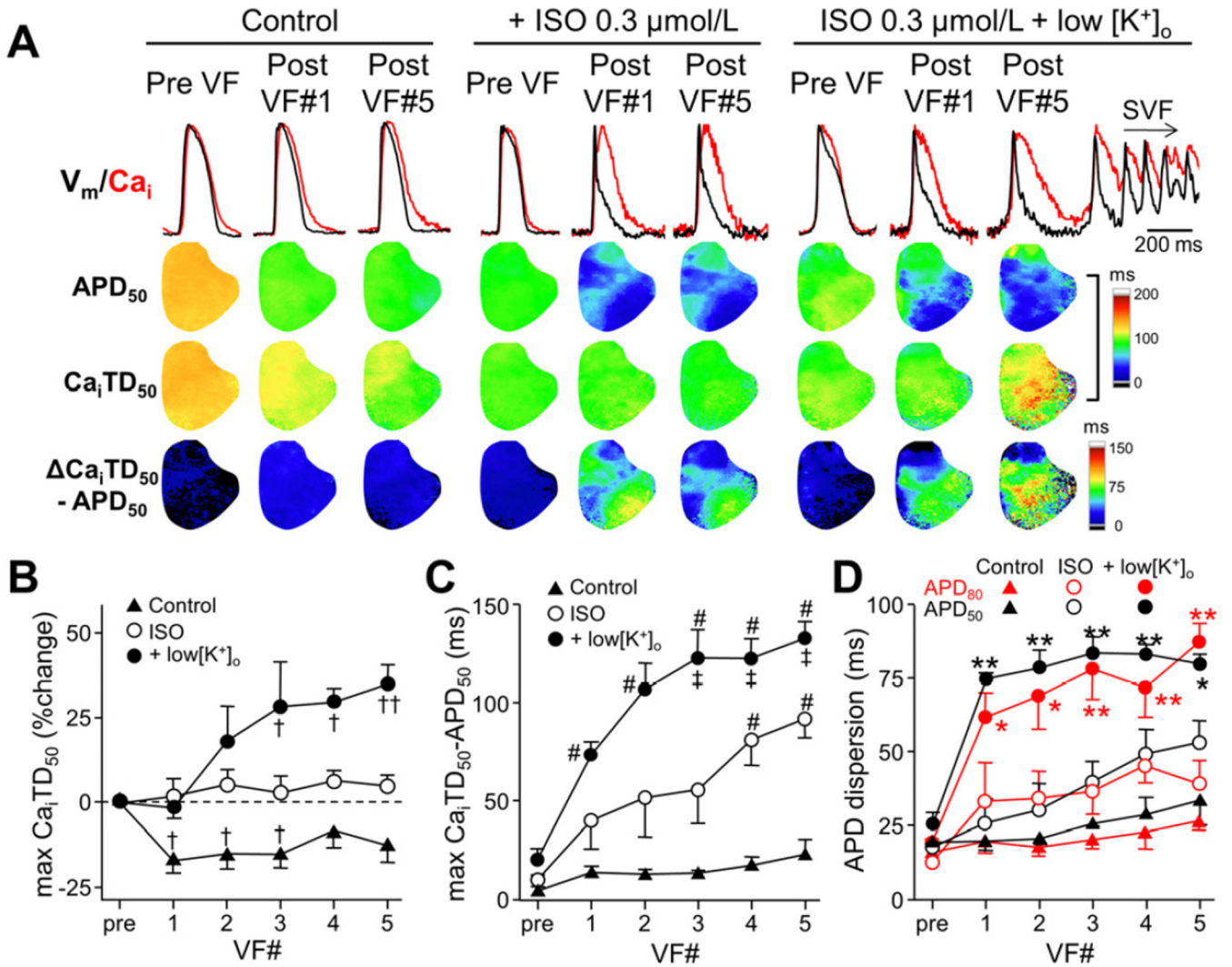


Figure 4.

APD and Ca_iTD after repeated VF episodes. **(A)** V_m and Ca_i tracings, APD_{50} maps, $\text{Ca}_i\text{TD}_{50}$ maps, and $\text{Ca}_i\text{TD}_{50} - \text{APD}_{50}$ maps are shown. ISO = isoproterenol. **(B)** %Changes in maximal $\text{Ca}_i\text{TD}_{50}$ after repeated VFs ($n=5$). $\dagger P < 0.05$; $\dagger\dagger P < 0.01$ versus pre-VF. **(C)** Effect of repeated VFs on the maximal $\text{Ca}_i\text{TD}_{50} - \text{APD}_{50}$ ($n=5$). $\# P < 0.01$ versus control; $\ddagger P < 0.05$ versus ISO. **(D)** Changes in APD dispersion at 50% and 80% repolarization. APD dispersion was defined as the difference between maximal and minimal APDs in the mapped area. $* P < 0.05$; $** P < 0.01$ versus control.

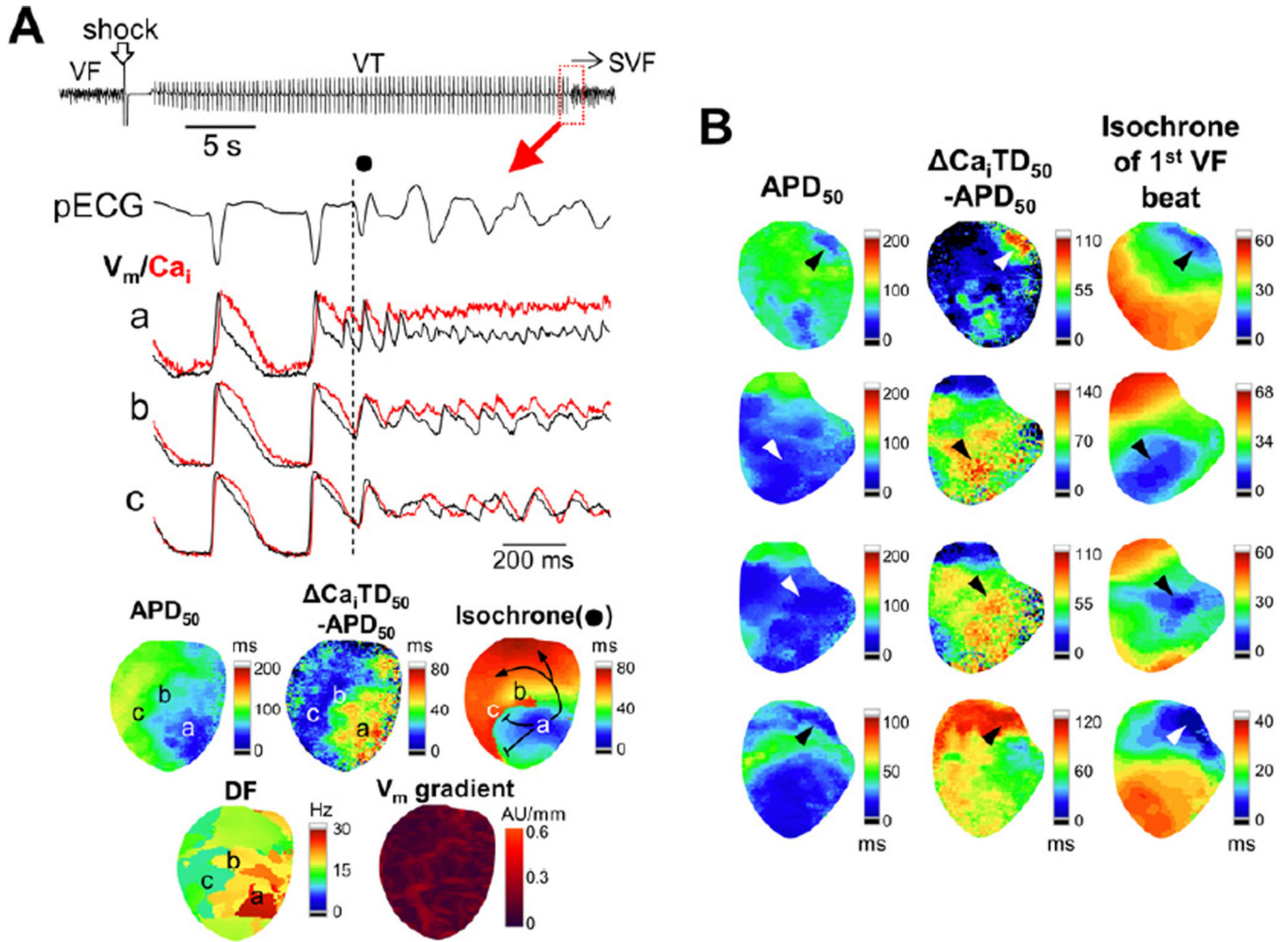


Figure 5.

Optical mapping of SVF. (A) Initiation of SVF. The timing of the QRS onset for the first VF beat (filled circle) is indicated with a dashed vertical line. V_m and Ca_i tracings were recorded at sites in the alphabets on the maps. APD_{50} , $Ca_iTD_{50}-APD_{50}$, and V_m gradient maps were constructed for the last VT beat and isochronal map for the first SVF beat. Dominant frequency (DF) map shows DF distribution during SVF. Note that the SVF initiation site (site (a)) has a high $Ca_iTD_{50}-APD_{50}$ and a high DF during VF. (B) Relationship among the first activation site of SVF (arrowheads), APD_{50} , and $Ca_iTD_{50}-APD_{50}$ in 4 different episodes. Note that the maximal $Ca_iTD_{50}-APD_{50}$ sites coincide the VF initiation site.

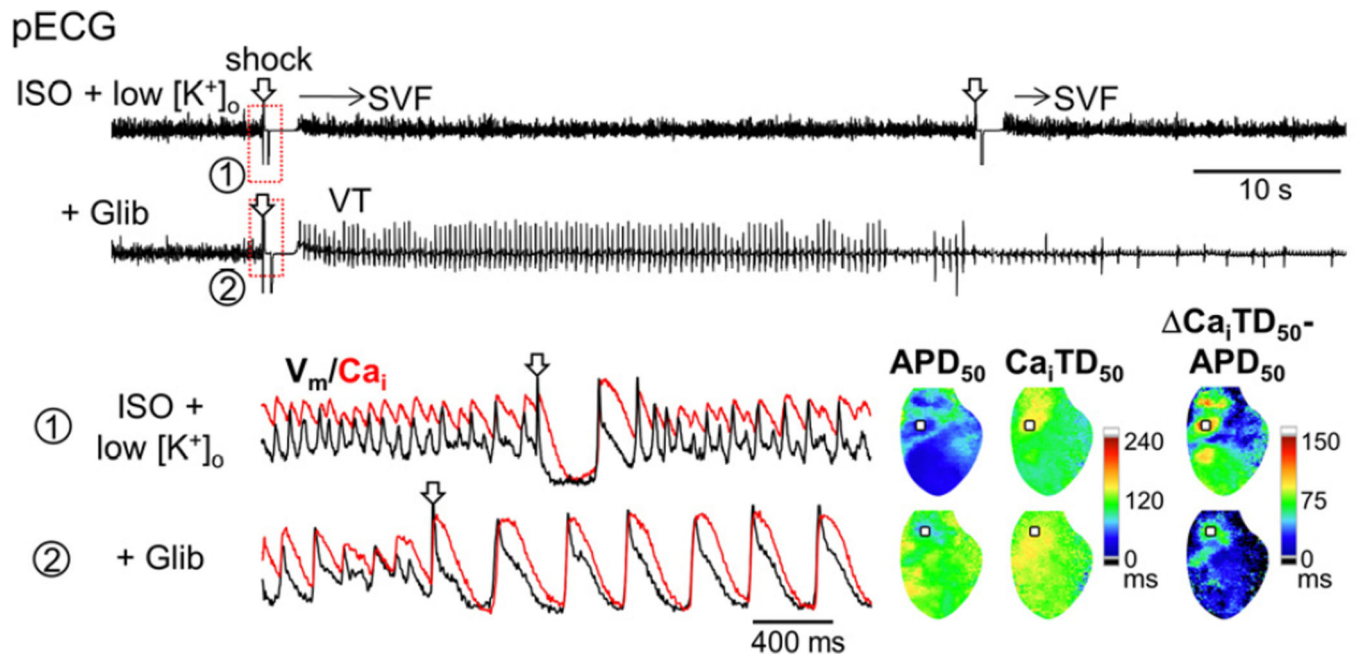


Figure 6.

Glibenclamide (Glib) terminates ES. Pseudo-ECGs (upper panels) and V_m/Ca_i tracings at the maximal Ca_iTD_{50} - APD_{50} site (squares) before and after addition of Glib are shown. Note that Glib prolonged the post-defibrillation APD_{50} , which decreased Ca_iTD_{50} - APD_{50} and prevented SVF.

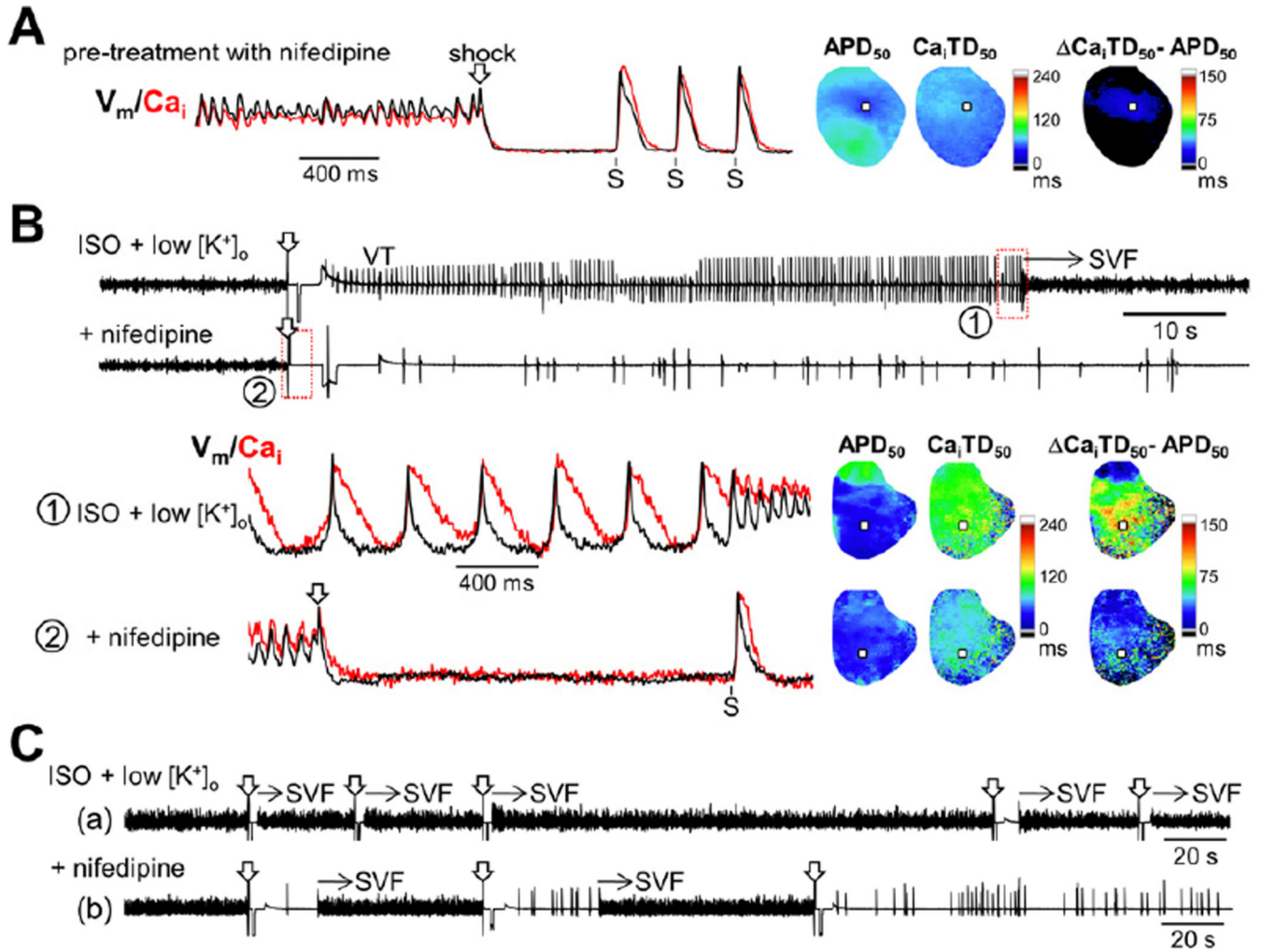


Figure 7.

Effects of $I_{Ca,L}$ blockade. **(A)** No VT or SVF occurred after multiple induced-VFs in the hearts pre-treated with nifedipine. Ventricular pacing (S) after shock was performed to assess APDs. V_m and Ca_i tracings were obtained at the minimal APD site on the maps for the first paced beat (squares). **(B)** Nifedipine suppressed VT and SVF when administered for ES with a long-lasting intervening VT. Optical tracings were recorded at the maximal $Ca_iTD_{50}-APD_{50}$ site (squares) before (upper panels) and after (lower panels) treatment with nifedipine. **(C)** (Upper panel) Pseudo-ECG during ES with immediate recurrences of SVF. (Lower panel) Successful termination of ES with nifedipine and repeated shocks.

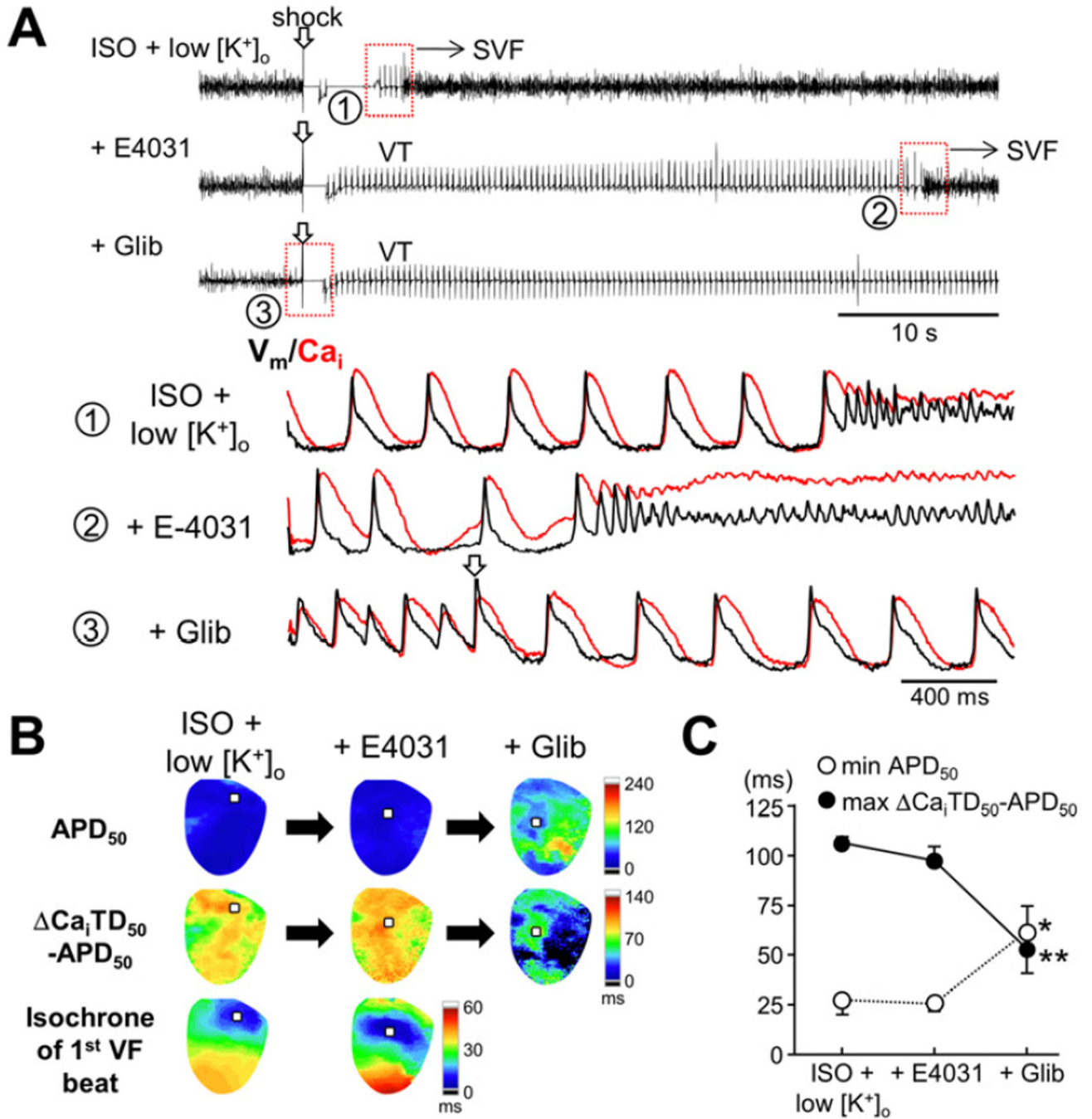


Figure 8.

Failure to terminate ES with I_{Kr} blockade. (A) Pseudo-ECGs and optical tracings during ES before and after I_{Kr} blockade with E-4031, and addition of glibenclamide (Glib). (B) APD_{50} maps, $Ca_iTD_{50} - APD_{50}$ maps, and isochrones of the 1st VF beat. Optical tracings in panel A were obtained at the maximal $Ca_iTD_{50} - APD_{50}$ sites (squares on each map). (C) Changes in the minimal APD_{50} and the maximal $Ca_iTD_{50} - APD_{50}$ (n=4). * $P < 0.05$; ** $P < 0.01$.